European Journal of Ophthalmology / Vol. 13 Suppl. 3, 2003 / pp. S44-S56

Pharmacological strategies to block rod photoreceptor apoptosis caused by calcium overload: a mechanistic target-site approach to neuroprotection

D.A. FOX[1,2,3], A.T. POBLENZ[2], L. HE[2], J.B. HARRIS[1], C.J. MEDRANO[1]

[1]College of Optometry
[2]Department of Biology and Biochemistry
[3]Department of Pharmacology and Pharmaceutical Sciences, University of Houston, Houston, Texas - USA

PURPOSE: *Photoreceptor apoptosis and resultant visual deficits occur in humans and animals with inherited, and disease-, injury- and chemical-induced retinal degeneration. Our aims were three-fold: 1) to determine the kinetics of rod apoptosis and Ca^{2+} overload in $Pde6b^{rd1}$ mice and developmentally lead-exposed rats, 2) to establish a pathophysiologically-relevant model of Ca^{2+} overload/rod-selective apoptosis in isolated rat retina and 3) to examine different mechanistic based neuroprotective strategies that would abrogate or mollify rod Ca^{2+} overload/apoptosis.*

METHODS: *Retinal morphometry and elemental calcium content ([Ca]) determined the kinetics of rod apoptosis and Ca^{2+} overload. A multiparametric analysis of apoptosis including rod [Ca], a live/dead assay, rod oxygen consumption, cytochrome c immunoblots and caspase assays was combined with pharmacological studies of an isolated rat retinal model of rod-selective Ca^{2+} overload/apoptosis.*

RESULTS: *Ca^{2+} overload preceded rod apoptosis in mice and rats, although the extent and kinetics in each differed significantly. The isolated rat model of rod Ca^{2+} overload/apoptosis showed that blockade of Ca^{2+} entry through rod cGMP-activated channels with L-cis diltiazem was partially neuroprotective, whereas blockade of Ca^{2+} entry into rods through L-type Ca^{2+} channels with D-cis diltiazem or verapamil provided no protection. Inhibition of the mitochondrial Na^{+}/Ca^{2+} exchanger with D-cis diltiazem provided no protection. CsA and NIM811, mitochondrial permeability transition pore (mPTP) inhibitors, blocked all Ca^{2+}-induced apoptosis, whereas the caspase-3 inhibitor DEVD-fmk only blocked the downstream cytochrome c-induced apoptosis.*

CONCLUSIONS: *The successful pharmacological neuroprotective strategies for rod Ca^{2+} overload/apoptosis targeted the rod cGMP-activated channels or mPTP, but not the rod L-type Ca^{2+} channels.* Eur J Ophthalmol 2003; 13 (Suppl. 3): S 44-S56

KEY WORDS. *Retinal degeneration, Rod photoreceptors, Apoptosis, Ca^{2+} overload, Mitochondria, Neuroprotection*

Accepted: December 18, 2002

1120-6721/S44-13$06.50/0

Part of this original work was presented by Dr. Donald A. Fox on February 15, 2002 at the International Workshop on Neuroprotection in Ophthalmology: From Basic Research to New Therapeutic Strategies for Eye Disease; University of Roma Tor Vergata, Roma, Italy

INTRODUCTION

Impairment and loss of vision resulting in blindness are major human health problems. The majority of these cases involve the photoreceptors or retinal ganglion cells (1). For example, rod photoreceptor cell apoptosis occurs in humans and animals with different forms of inherited retinal degenerations, cancer-associated retinopathy (CAR), Batten's disease, lead exposure during development and adulthood, chemical or drug exposure, mild hypoxic-ischemia injury, or light-induced damage (1-12; also see Tab. I and references therein). Alterations in the expression, structure and/or function of photoreceptor visual transduction cascade proteins, visual cycle proteins, outer segment disc structural proteins, ATP utilizing transport proteins, transcription factors and mitochondrial proteins underlie most of the photoreceptor apoptosis in retinal degenerations (8, 10, 16, 37, 38). Although the mutation(s) or upstream initiators of photoreceptor cell death may be known and characterized (8,10,13,14, 16, 37-40; see Tab. I), the exact molecular mechanism(s) of photoreceptor apoptosis are mostly unknown.

The kinetics of neuronal cell death in 12 different models of inherited photoreceptor degeneration and of photoreceptor dysfunction in patients with retinitis pigmentosa and cone-rod dystrophy have been modeled. Results show that rod cell death and rod electroretinographic functions - in all except the rd1 mouse (allele symbol: $Pde6b^{rd1}$) - follow an exponential decline that results from either a constant or decreasing risk of cell death with time (41). This suggests that a single stochastic biochemical event triggers photoreceptor cell death. Ca^{2+} overload, Bax or the generation of reactive oxygen species (ROS) in photoreceptors could initiate and/or amplify the apoptotic process (14, 41, 42). The findings from this kinetic model of cell death have important implications and ramifications in the therapeutic treatment and outcome of neurodegenerative retinal and neuronal diseases.

Numerous studies report that a sustained elevation of intracellular [Ca^{2+}] ($[Ca^{2+}]_i$) results in apoptotic cell death (14, 43, 44). During the effector phase of apoptosis the mitochondrial permeability transition pore (mPTP) is irreversibly opened by sustained increases in matrix Ca^{2+} leading to mitochondrial depolarization, release of cytochrome c, activation of caspases, chromatin cleavage and apoptotic nuclear morphology (44-47). Mutations (13, 48) or chemical-induced (Pb^{2+}) inhibition of rod-specific cyclic GMP phosphodiesterase (cGMP PDE: Pde6) (27, 28) should result in increased or prolonged opening of the rod cGMP-gated channel, rod photoreceptor Ca^{2+} overload and eventually rod cell death (13, 14, 49, 50). Recently, Frasson et al (50) reported that the Ca^{2+}-channel blocker

TABLE I - HUMAN AND ANIMAL RETINAL DEGENERATIONS INVOLVING PHOTORECEPTOR Ca^{2+} OVERLOAD

Retinal photoreceptor degeneration		
Classification	**Initiating event**	**References**
arRP	Mutations in gene for β-subunit of rod cGMP PDE	10,13-16
arRP	Mutations in gene for α-subunit of rod cGMP PDE	17,18
RP-like	Mutation in gene for γ-subunit of rod cGMP PDE	19
adCD, adCRD	Mutations in gene for GCAP1	20-22
Batten's Disease	Mutations in CLN3 gene	23,24
CAR	Autoantibodies and monoclonal antibodies to recoverin	2,9
Lead exposure	Inhibition of rod cGMP PDE and Na^+, K^+-ATPase	14,25-29
Na,K-ATPase KO	β2 subunit null mutant or β2/β1 knock-in mice	30-32
Ischemia-Reperfusion	Oxygen deprivation	33-35
Photic Injury	Photon absorption	4,36

ad= Autosomal dominant; ar= Autosomal recessive; CAR= Cancer-associated retinopathy; CD= Cone dystrophy; cGMP PDE= Cyclic GMP phosphodiesterase; CRD= Cone-rod dystrophy; GCAP1= Guanylate cyclase activating protein 1; KO= Knock out; RP= Retinitis pigmentosa

TABLE II - BLOOD (µg/dl) AND RETINAL (ppm) LEAD CONCENTRATIONS IN CONTROLS AND RATS EXPOSED TO LEAD ONLY DURING EARLY POSTNATAL DEVELOPMENT [a]

Age (days)	Tissue	Control	Lead-Exposed
7	Blood	0.7 ± 0.5	40.3 ± 5.9[c]
	Retina	0.01 ± 0.01	0.18 ± 0.03[c]
14	Blood	1.2 ± 0.9	49.9 ± 6.8[c]
	Retina	0.01 ± 0.01	0.27 ± 0.03[c]
21[d]	Blood	1.4 ± 1.1	59.0 ± 8.0[c]
	Retina	0.02 ± 0.01	0.61 ± 0.04[c]
45	Blood	4.4 ± 2.2	19.0 ± 8.0[c]
	Retina	0.03 ± 0.02	0.18 ± 0.05[c]
90[d]	Blood	5.4 ± 2.4	6.8 ± 2.1
	Retina	0.04 ± 0.01	0.12 ± 0.02[b]

[a] Values for lead represent the mean ± SEM for 6-14 rats per lead treatment condition as described under Materials and Methods

[b] Significantly different from control at $p < 0.05$

[c] Significantly different from control at $p < 0.02$

[d] Blood and retinal lead values at PN21 and PN90 previously reported (25)

D-cis diltiazem (51), a weak inhibitor of the rod cGMP-gated conductance (52), partially rescued the degenerating rod photoreceptors of rd1 mice retinas with a mutation in the beta-subunit of the Pde6 gene ($Pde6b^{rd1}$ mice). They suggested that the rescue resulted from blocking L-type Ca^{2+} channels in rods. In marked contrast, other investigators using $Pde6b^{rd1}$ mice and the same D-cis diltiazem treatment protocol found no rescue (53). Moreover, Pearce-Kelling et al (54) found no rescue by D-cis diltiazem in dogs with a similar mutation in the Pde6 gene ($Pde6b^{rcd1}$) and Bush et al (55) found no rescue of rod degeneration by D-cis diltiazem in rats with a Pro23His rhodopsin mutation. To date, no such rescue experiments have been performed in developmentally lead-exposed rodents or in *in vitro* retinal experiments modeling these rod degenerations.

The aims of these experiments were threefold: 1) to determine the extent and kinetics of rod cell death and Ca^{2+} overload in $Pde6b^{rd1}$ mice and developmentally lead-exposed rats in order to obtain data for an *in vitro* model of Ca^{2+} overload, 2) to establish a pathophysiologically-relevant model of Ca^{2+} overload in isolated whole rat retina to determine the mechanism of rod cell death, and 3) to examine the role of five different sites of action using selected pharmacological agents that could modify Ca^{2+} flux, $[Ca^{2+}]_i$ and/or apoptosis by different mechanisms in order to develop rational pharmacological approaches that would abrogate or mollify photoreceptor cell death.

MATERIALS AND METHODS

Experimental animals

All experimental and animal care procedures were in compliance with the principles of the American Physiological Society and the NIH Guide for the Care and Use of Laboratory Animals (NIH Publication No. 85-23, 1985). Animal care and maintenance, the environmental lighting conditions and the developmental lead protocol in rats were described previously (25). Briefly, pregnant Long-Evans hooded dams were randomly divided into two groups: control and lead-exposed. On the day of birth (postnatal day 0: PN0) the tap water used for the lead-exposed group was replaced by 0.20% lead acetate solution (1090 ppm lead) and the litter was culled to eight pups. The lead drinking solution was provided *ad libitum* to dams throughout lactation so that the pups were exposed to lead only via the mother's milk from PN0 to weaning (PN21). Litter sizes were maintained at eight pups throughout lactation by cross-fostering. At weaning the pups were transferred to hanging stainless steel cages, fed Purina chow and tap water *ad libitum*. Blood and retinal lead concentrations were determined at PN7, 14, 21, 45 and 90 as described (25).

Retinas were obtained from developing and adult C57 BL/6N normal mice (+/+) and C57 BL/6J homozygous retinal degeneration (rd1) mice (allele symbol: $Pde6b^{rd1}$). Mice homozygous for the rd1 mutation have an almost complete retinal degeneration early during postnatal development due to a nonsense mutation in exon 7 of the Pde6b gene encoding the β-subunit of rod-specific cGMP PDE (48). Mice were weaned on PN21 and litter sizes were maintained at six pups throughout lactation by cross-fostering. The $Pde6b^{rd1}$ mice were kindly provided by Dr. Paul Overbeek at Baylor College of Medicine, Houston, TX.

Histology, confocal microscopy and retinal calcium content

Counts of rod and cone cells (nuclei) were made in four retinal quadrants in PN7-PN45 rats and mice (3-5 animals per age): posterior pole (central retina) and far periphery of the superior and inferior temporal quadrants as described (3, 56).

Fluo-3 Ca^{2+} imaging and confocal laser scanning microscopy were used as described (44) to localize the distribution and to determine the relative concentrations of free Ca^{2+} in dark- and light-adapted adult rat retinas (n = 2-3 retinas per condition). Retinas were mounted photoreceptor side down, scanned every 2 µm, and following the experiments the 90-100 images were aligned and stacked using the 3-dimensional software program in NIH Image (Version 1.62). Dark-adapted retinas were incubated at 37°C in physiological Tris buffer (30 mM Tris-HCl, 120 mM NaCl, 5 mM KCl, 3 mM $MgCl_2$, 1 mM free Ca^{2+}, 10 mM glucose, pH 7.4, 310 mOsm). After scanning, retinas were exposed to a rod-saturating light stimulus and the procedure was repeated.

Retinal elemental Ca^{2+} ([Ca]) was measured in 3-5 rats and mice from each treatment group at each age as described (26, 57). To determine the extent of rod photoreceptor Ca^{2+} overload in different buffers, rod outer-inner segment [Ca] was measured as described (57, 58).

Rat retinal incubations

Rat neural retinas were isolated and used essentially as described (44, 58, 59). Briefly, each retina was incubated at 37°C for 15 minutes in 10 ml of Tris buffer (30 mM Tris-HCl, 120 mM NaCl, 5 mM KCl, 3 mM $MgCl_2$, with or without 1 mM free Ca^{2+}, 10 mM glucose, pH 7.4, 310 mOsm) with or without 0.5 mM 3-isobutyl-1-methylxanthine (IBMX). IBMX was used to partially inhibit rod cGMP PDE (27, 49) in order to produce Ca^{2+} overload similar to that observed in $Pde6b^{rd1}$ mice and developmentally lead-exposed rats (Fig. 1). There were no differences, on any measure, between control retinas incubated in the absence of Ca^{2+} and with or without IBMX, so the data for these two conditions were combined and presented as control buffer.

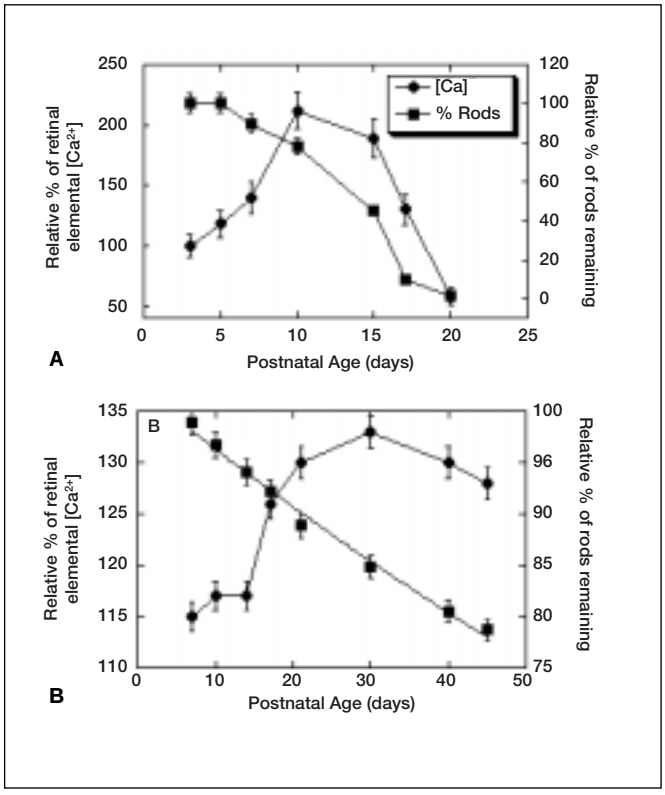

Fig. 1 - *Kinetics of rod photoreceptor degeneration and Ca^{2+} overload in (**A**) $Pde6b^{rd1}$ mice retinas and (**B**) developmentally lead-exposed rat retinas. The kinetics of the apoptotic rod cell loss in the $Pde6b^{rd1}$ mice is characterized by a sigmoidal decline indicating an increasing risk of rod cell death with time and in the lead-exposed rats is characterized by an exponential decline ($y = 102.3e^{-0.006}$; r = 0.99) indicating a constant risk of rod cell death with time (41). Note that the increase in elemental [Ca^{2+}] ([Ca]) precedes the onset and peak of rod apoptosis in both animal models and that the level of Ca^{2+} overload correlates with the extent of rod cell loss. Percent values represent the mean ± SEM of whole retinal [Ca] for 3-5 dark-adapted mice and rats per treatment group compared to age-matched controls as described (26, 57).*

Pharmacological experiments

Five different sites of action were examined using pharmacological agents at the indicated concentrations. L-cis diltiazem (25 µM) was used to block the rod cGMP-activated conductance (53) since it is a weak inhibitor of L-type Ca^{2+} channels (51) and a very weak inhibitor of the mitochondrial Na^+/Ca^{2+} exchanger (60) present in rods (57). D-cis diltiazem (CGP 37157™ or Cardizem™: 25 µM) was used to block the mitochondrial Na^+/Ca^{2+} exchanger (61, 62) and L-type

Ca^{2+} channels (51), although it is also a weak inhibitor of the rod channel (53). Verapamil (100 µM) was primarily used to block voltage-sensitive Ca^{2+} channels (51) because it does not block the rod cGMP-activated conductance (53) and it is a weak inhibitor of the mitochondrial Na^+/Ca^{2+} exchanger (63). Cyclosporin A (CsA: 5 µM) and NIM811 (n-methyl-4-isoleucine-cyclosporin: 5 µM), a nonimmunosuppressive cyclosporin analog (64), were used to inhibit the mPTP (44, 47, 65). FK506 (100 nM) was used as a control for CsA because both inhibit calcineurin but FK506 does not inhibit the mPTP (47, 66). DEVD-fmk (1 nM) was used to preferentially inhibit the group II caspases (67). All drugs were added to the buffers. The vehicle controls, either DMSO or ethanol, exhibited no effects on any measure.

Rod photoreceptor oxygen consumption (QO_{PR})

QO_{PR} of individual adult rat retinas (n = 3-5 retinas per condition), incubated in Tris buffers, was determined polarographically and recorded in the dark or during presentation of a rod-saturating light adapting stimulus as described (58, 59).

Detection and quantification of apoptosis, caspase assay and cytochrome c immunoblot

To quantify the number of apoptotic and necrotic cells and to determine the location and type(s) of retinal cells undergoing apoptosis, retinas incubated in Tris buffers (n = 3-5 retinas per condition) were stained with acridine orange/ethidium bromide (AO/EtBr) as described (44) and viewed on an Olympus IX-70 inverted microscope equipped for epifluorescence. All layers of the central and mid-peripheral retinas were scanned and stained nuclei were counted in ten visual fields in four different retinal areas using stereological procedures. Values represent means ± SEM of the combined number of early and late apoptotic nuclei per mm^2 of retina.

Caspase-3 activity was measured using DEVD-pNA as described (44). Absorbance was measured at 405 nm. The arbitrary values are presented as means ± SEM for 3-5 experiments per condition.

To detect and quantify the cytosolic cytochrome c (n = 3-4 experiments per treatment), cytosolic (S100) fractions were prepared, assays were performed and the intensities of the bands on the immunoblots were quantified using NIH Image software as described (44). Immunoblot analysis was carried out using an ECL Plus kit (Amersham) according to manufacturer's instructions. To confirm that there was no mitochondrial contamination in the cytosolic fractions, immunoblots used for cytochrome c detection were stripped and examined for cytochrome oxidase IV as described (44).

Statistical analysis

All group data were studied using the appropriate analysis of variance (ANOVA) and *post hoc* multiple comparisons using Tukey's Honestly Significant Difference test (StatView, Abacus Concepts, Inc., Berkeley, CA). All statistical analysis was performed on untransformed data. All data is presented as means ± SEM. For all data, the difference from controls was regarded as significant if $p < 0.05$.

RESULTS

Kinetics of rod photoreceptor loss and calcium overload in $Pde6b^{rd1}$ mice and developmentally lead-exposed rats

As previously reported, rod photoreceptors of $Pde6b^{rd1}$ mice undergo a massive and almost complete apoptotic cell death between PN7 and PN21 (6, 7, 13; Fig. 1A). The kinetics of this apoptotic rod cell loss is characterized by a sigmoidal decline indicating an increasing risk of rod cell death with time (41; Fig. 1A). Approximately two days prior to the onset of rod apoptosis the retinal [Ca] of these mice begins to increase (120-140% of control). This increase in [Ca] continues throughout the period of massive rod apoptosis peaking at ~200% of the age-matched control value on days PN10-PN15: the period during which ~50% of the rods are lost (Fig. 1A). By PN21, 95-98% of the rods in the $Pde6b^{rd1}$ mice are lost and the retinal [Ca] is ~60% of the age-matched control value.

A similar correlation between an early rise in retinal [Ca] and [Pb] and the onset of apoptotic rod cell death (3, 8) was observed in lead-exposed rats (Fig. 1B, Tab. II). However, there are three distinguishable and important differences between the results in the

rat and mouse models of clinically relevant retinal degeneration. First, the kinetics of the lead-induced apoptotic rod-selective cell loss, that occurs over a 50 day period in the rats, is characterized by an exponential decline indicating a constant risk of rod cell death with time (41; Fig. 1B). Second, the total number of rods lost in the rats is ~22% (3). Third, early during development the retinal [Ca] is 115-120% of the age-matched control value and then it reaches a plateau of ~130% of the age-matched values from PN17 to PN45: the period when ~60% of the apoptotic rod cell death occurs in the rat (Fig. 1B). Overall, the lead-induced model of rod cell death is consistent with most models and cases of slow progressive retinal and neuronal degenerations (41).

Confocal localization of calcium during dark and light adaptation

During dark adaptation the $[Ca^{2+}]_i$ in rods is considerably higher (400-500 nM) than during light adaptation (50-80 nM) (68, 69). We utilized fluo-3 Ca^{2+} imaging and confocal laser scanning microscopy (44) to ascertain whether the rods of isolated intact rat retina incubated in Tris buffer containing 1 mM Ca^{2+} maintain their normal regulation of $[Ca^{2+}]_i$ during dark and light adaptation and to examine the relative distribution of $[Ca^{2+}]_i$ in the dark- and light-adapted rat retina. During dark adaptation, the fluo-3 fluorescence was localized almost exclusively in the outer retina (i.e., photoreceptors) as evidenced by the high intensity of the dye in several rods (Fig. 2). In the light-adapted retina, the Ca^{2+}-induced fluo-3 fluorescence level in the outer retina was markedly decreased. The fluo-3 fluorescence was consistently lower in the inner than outer retina during both dark and light adaptation (Fig. 2). These findings show that the rod photoreceptors in the isolated rat retina maintain their normal physiological regulation of Ca^{2+} fluxes.

Retinal Ca^{2+} overload and apoptotic rod cell death: strategies for cytoprotection

To establish an *in vitro* model of Ca^{2+} overload similar to that observed *in vivo* (Fig. 1), the rod [Ca] from light-adapted retinas was measured after incubation in different buffers. The rod [Ca] content from retinas incubated in control buffer in the absence of added Ca^{2+} was ~25 ppm and this only increased 7-8% in the presence of 1 mM Ca^{2+}. Rod [Ca] in buffer containing 1 mM Ca^{2+} and IBMX increased ~30% compared to the Ca^{2+}-free buffer. This buffer was used to produce Ca^{2+} overload in all subsequent experiments as the percent [Ca] increase was similar to that measured in rat retinas during developmental lead exposure (Fig. 1B).

AO/EtBr staining was used to distinguish between viable, early apoptotic, late apoptotic and necrotic cells (44). All early and late apoptotic nuclei were identified as rod photoreceptor cells as determined by their localization within the outer nuclear layer and nuclear diameter. Light-adapted retinas incubated in physiological control buffer (CON) in the absence or presence of 1 mM Ca^{2+} had 20-25 apoptotic rods/mm^2 of retina (Fig. 3). The number of apoptotic rods in retinas incubated in buffer containing 1 mM Ca^{2+} and IBMX increased over 5-fold. Electron microscopy confirmed that the Ca^{2+}-induced retinal cell death in the presence of IBMX was rod-specific and apoptotic (data not shown). L-cis diltiazem partially blocked this Ca^{2+}-induced increase in rod apoptosis, whereas D-

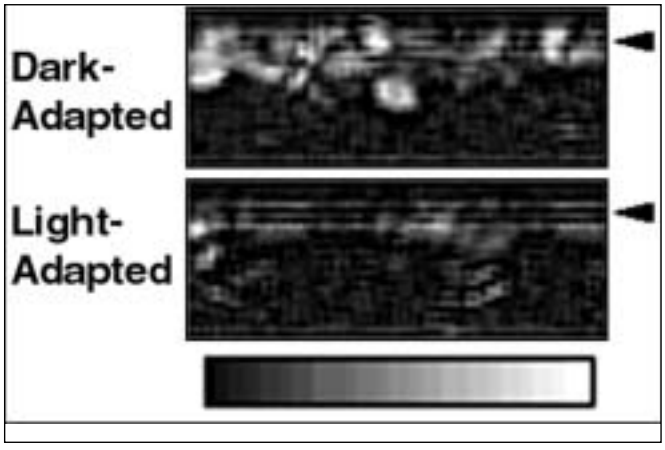

Fig. 2 - *Fluo-3 Ca^{2+} imaging and confocal laser scanning microscopy of dark-adapted and light-adapted rat retinas. Fluo-3 Ca^{2+} imaging and confocal laser scanning microscopy were used as described (44). Dark-adapted retinas were incubated at 37°C in physiological Tris buffer containing 1 mM free Ca^{2+} as described in the Methods. The retinas were whole mounted photoreceptor side down and examined with the confocal laser scanning microscopy following fluo-3 loading as described (44). The images were processed using NIH Image Software. The arrowheads mark the outer retinal (photoreceptor) region. The fluo-3 signal was localized mainly to the photoreceptors during both adaptation states. These images are representative of 2-3 retinas for each adaptation condition.*

cis diltiazem and verapamil had no effect (Fig. 3). These results suggest that excess Ca^{2+} enters the rod through the cGMP-gated channel, and not through the L-type Ca^{2+} channel in the rod inner segment or synaptic terminal (71). NIM811, CsA and DEVD-fmk completely blocked the Ca^{2+}-induced increase in rod apoptotic cell death, but FK506 had no effect (data not shown). These results confirm and extend our earlier findings (44) that pathophysiologically relevant levels of Ca^{2+} overload selectively kill rod photoreceptors by opening the mPTP and activating the cytochrome c-caspase cascade of apoptosis. The number of necrotic cells did not vary with any incubation condition: ~2 necrotic cells/mm^2 of retina.

Retinal Ca^{2+} overload decreases photoreceptor respiration (QO_{PR})

The above results, in combination with our previous data showing a concentration-dependent inhibition of retinal mitochondrial respiration by Ca^{2+} (57), suggest that retinal Ca^{2+} overload decreases rod mitochondrial function. To assess the overall bioenergetics of rod photoreceptors during Ca^{2+} overload, we measured QO_{PR} during dark and light adaptation in the absence and presence of various pharmacological inhibitors (Fig. 4). In control adult rat retinas incubated in physiological buffer containing 1 mM Ca^{2+}, the dark-adapted QO_{PR} was 1.8 µmole O_2 mg dry wt^{-1} hr^{-1} and it decreased 37% during light adaptation (Fig. 4). Relative to dark- and light-adapted controls, the QO_{PR} of retinas during Ca^{2+} overload (Ca^{2+} plus IBMX buffer) decreased 31% and 15%, respectively. Interestingly, L-cis diltiazem blocked the Ca^{2+}-induced decrease in QO_{PR} during light adaptation when fewer rod cGMP channels are open (53) and the apoptosis assays were performed, but not during dark adaptation. D-cis diltiazem had no neuroprotective effect. NIM811 and CsA (data not shown) blocked the Ca^{2+}-induced decrease in QO_{PR} during both dark and light adaptation (Fig. 4), whereas FK506 and verapamil had no cytoprotective effect (data not shown). These results suggest that Ca^{2+} inhibits rod mitochondrial respiration by opening the mPTP and releasing cytochrome c.

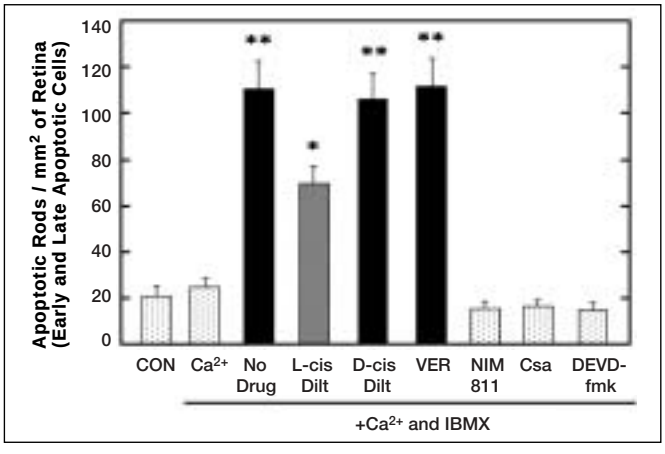

Fig. 3 - *The Ca^{2+} overload-induced rod-selective apoptosis is not blocked by D-cis diltiazem or verapamil, but is blocked by L-cis diltiazem, NIM811, CsA and DEVD-fmk. The number of combined early and late apoptotic rod cells for each treatment condition, identified and defined by AO/EtBr staining as described (44), is presented as the mean ± SEM of the number of apoptotic rod cells per mm^2 of retina for 3-5 retinas for each treatment condition. Retinas were incubated in control buffer in the absence of Ca^{2+} (CON), or in buffers containing Ca^{2+} and IBMX plus vehicle (No Drug), either 25 µM L-cis diltiazem (Dilt), 25 µM D-cis diltiazem (Dilt), 100 µM verapamil (VER), 5 µM NIM811, 5 µM CsA or 1 nM DEVD-fmk. All values with asterisks are significantly different from controls at: * $p < 0.05$ and ** $p < 0.02$.*

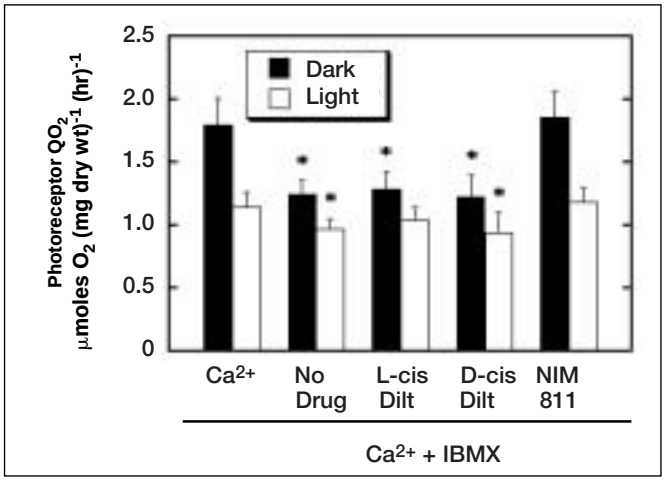

Fig. 4 - *The Ca^{2+} overload-induced decrease in photoreceptor oxygen (QO_{PR}) consumption during dark and light adaptation is partially blocked by L-cis diltiazem and blocked by NIM811. The photoreceptors were pharmacologically-isolated from the inner retina as described (58, 59). The retinas were incubated in control buffer in the presence of 1 mM free Ca^{2+} (Control) or in buffers containing Ca^{2+} and IBMX plus vehicle (No Drug) with either 25 µM L-cis diltiazem or 5 µM NIM811. Each retina was used for only one experiment. Values represent the mean ± SEM for 3-5 retinas per each measure. All values with asterisks are significantly different from controls at: * $p < 0.05$.*

The Ca^{2+}-induced cytochrome c release is completely inhibited by CsA, but not by DEVD-fmk or L-cis diltiazem

To directly determine whether cytochrome c was released during Ca^{2+} overload and whether selected pharmacological agents could block its release, we examined the S100 fraction of retinas following various incubations (Fig. 5). Retinas incubated in Ca^{2+} plus IBMX buffer (control) had a significant amount of cytochrome c in the cytosolic fraction (Fig. 5: lane 1). DEVD-fmk did not change the amount of cytochrome c released into the cytosolic fraction (Fig. 5: lane 2; 96 ± 6% of control), showing that activation of Group II caspases during rod Ca^{2+} overload is not required for cytochrome c release. L-cis diltiazem slightly decreased the amount of cytochrome c released (Fig. 5: lane 3; 81 ± 5% of control) consistent with its partial decrease in Ca^{2+}-induced rod apoptosis (Fig. 3 and 6). CsA (Fig. 5: lane 4) and NIM811 (data not shown) completely blocked cytochrome c release, whereas FK506 had no effect (data not shown), indicating that rod Ca^{2+} overload opened the mPTP (47). A mitochondrial fraction from control retinas was loaded as a positive control (Fig. 5: mito). The absence of cytochrome oxidase subunit IV in the cytosolic fractions (Fig. 5: lanes 1-4) reveals no contamination of mitochondria.

Caspase-3 was activated during Ca^{2+} overload

Because cytochrome c interacts with caspase-9 to activate the Group II executioner caspases (71), we determined if caspase-3 was activated during incubation with the different Ca^{2+} buffers. DEVD-pNA, which is selectively cleaved by caspase-3, -7 and -8 (72, 73), was used as a substrate. Our previous work demonstrated that procaspase-7 was present in the adult rat retina, but was not activated by Ca^{2+} plus Pb^{2+} and that caspase-8 was not involved in Ca^{2+} plus Pb^{2+}-induced pathway of rod apoptosis (44). Therefore, we interpret increased DEVDase activity as solely due to activation of caspase-3 by caspase-9. Control retinas incubated in the absence or presence of Ca^{2+} exhibited a minimal amount of caspase-3 activity (Fig.

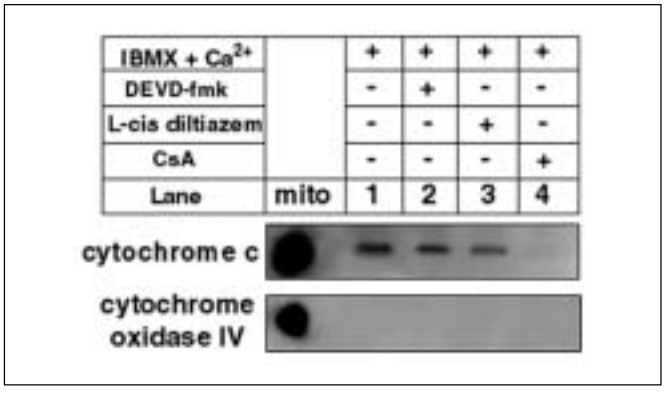

Fig. 5 - *The Ca^{2+} overload-induced cytochrome c release from mitochondria is partially blocked by L-cis diltiazem and blocked by CsA. The retinas were incubated in buffers containing Ca^{2+} and IBMX or Ca^{2+} and IBMX plus either 25 µM L-cis diltiazem or 5 µM CsA. Western Blot analysis and quantification of cytosolic cytochrome c and cytochrome oxidase IV were conducted as described (44). A representative blot shows that mitochondrial cytochrome c was released from retinas incubated with Ca^{2+} and IBMX (lane 1: control) and this release was not inhibited by 1 nM DEVD-fmk (lane 2: 96 ± 6% of control), partially inhibited by 25 µM L-cis diltiazem (lane 3: 81 ± 5% of control) or completely inhibited by 5 µM CsA (lane 4). A mitochondrial fraction (mito) was loaded as a positive control for cytochrome c. The absence of cytochrome oxidase IV in the cytosolic fractions (lanes 1-4) indicates no mitochondrial contamination. These blots are representative of 3-4 experiments for each treatment condition.*

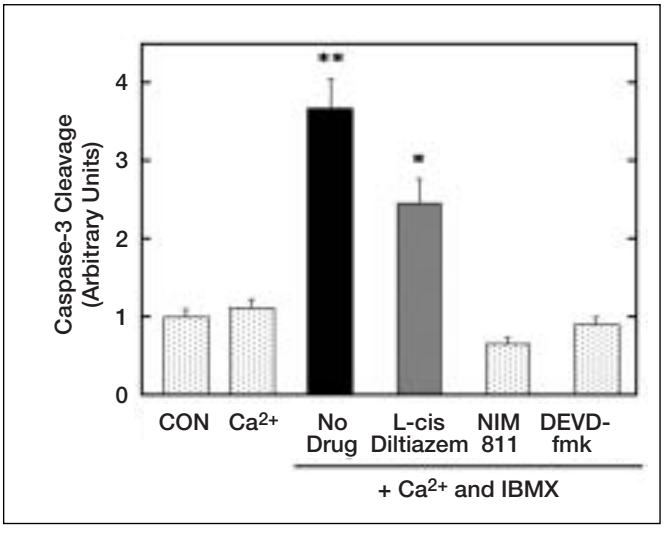

Fig. 6 - *The Ca^{2+} overload-induced activation of caspase-3 is partially blocked by L-cis diltiazem and blocked by NIM811 or DEVD-fmk. The retinas were incubated in buffers in the absence of Ca^{2+} (CON), containing 1 mM free Ca^{2+} (Ca^{2+}), or Ca^{2+} and IBMX with vehicle (No Drug) or either 25 µM L-cis diltiazem, 5 µM NIM811 or 1 nM DEVD-fmk and the caspase assay was performed as described (44). The arbitrary values represent the means ± SEM of 3-5 experiments for each treatment condition. All values with asterisks are significantly different from controls at: * $p < 0.05$ and ** $p < 0.02$.*

6). In contrast, retinas incubated in the Ca^{2+} plus IBMX buffer exhibited an ~4-fold increase in caspase-3 activity. The Ca^{2+}-induced increase in caspase-3 activity was inhibited by NIM811 and DEVD-fmk and slightly by L-cis diltiazem (Fig. 6), but not by FK506 (data not shown). The possibility that the increased caspase-3 activity resulted from a direct effect of Ca^{2+} on caspase-3 was eliminated because caspase-3 activity was inhibited by CsA and NIM811 and because high concentrations of EGTA (2.5 mM) and dithiothreitol (10 mM) were in the assay buffers. This is consistent with the findings that caspase activity is not affected by concentrations of Ca^{2+} below 100 mM (74).

DISCUSSION

The results from this study determined the kinetics of rod cell death and Ca^{2+} overload in two different animal models of developmental retinal degeneration, identified rod photoreceptors as selective targets of both *in vivo* and *in vitro* Ca^{2+} overload, delineated the major biochemical mechanisms in the cytochrome c-caspase apoptotic signaling cascade during Ca^{2+} overload, and identified potential neuroprotective strategies aimed at abrogating or mollifying the effects of Ca^{2+} overload. Moreover, the results clearly demonstrate that D-cis diltiazem, in contrast to L-cis diltiazem, provides no neuroprotection at any cellular level against low-to-moderate rod Ca^{2+} overload. The kinetics and degree of rod-selective apoptosis produced by pathophysiologically relevant concentrations of Ca^{2+} is similar to that observed in a wide variety of human and animal retinal degenerations where Ca^{2+} overload appears to have a fundamental role (Tab. I and references therein). Therefore, the concepts generated by these results may be useful to clinical therapy.

During developmental lead exposure, the rod [Pb] and [Ca] slowly increased and the kinetics of cell loss exhibited an exponential decline indicating a constant risk of apoptotic rod cell death with time. Similar kinetics of rod degeneration are seen in patients with inherited photoreceptor degenerations (41). Interestingly, it appears that developing rods and CNS neurons may be more sensitive to Ca^{2+} overload and other divalent cations such as Pb^{2+} and Hg^{2+} than mature rods or neurons (8,14,75,76), although some immature neurons appear more resistant to Ca^{2+} overload (77). The maximal increase of retinal [Ca] in lead-exposed rats was a modest 30%. However, in the $Pde6b^{rd1}$ mouse retina the maximum rod Ca^{2+} overload was ~7-fold higher (~200%) and apoptosis was rapidly and markedly increased: characterized by a sigmoidal decline indicating an increasing risk of rod cell death with time. In contrast to the kinetic pattern of rod apoptosis observed in the lead-exposed rats, the one in $Pde6b^{rd1}$ mouse retina has a much lower potential for therapeutic rescue (41). The rod selectivity is hypothesized to result from a sustained increase in rod [Ca] compared to cones (8, 44) because the $Na^{+}/Ca^{2+}(K^{+})$ exchanger in the rods is 8-10 times slower than in cones (78).

Pharmacological approaches, targeted overexpression of anti-apoptotic bcl-2 family members and survival/growth factor have been tried as neuroprotectants in animal models of rod photoreceptor degeneration and in isolated neurons exhibiting these two different kinetic patterns of apoptosis. The former two have specifically approached the idea of blocking or diminishing Ca^{2+} overload. The results to date have been equivocal in rods and neurons where there is an increasing risk of cell death associated with cumulative damage due to a sustained Ca^{2+} overload. In rods or neurons with sustained Ca^{2+} overload the mPTP will stabilize in the high-conductance open state such that the inner mitochondrial membrane will permeabilize causing an irreversible decrease in mitochondrial membrane potential, loss of ATP, swelling and release of pro-apoptotic proteins into the cytosol, and activation of the apoptotic cascade (45-47). Normally, rod mitochondria contain low levels of Ca^{2+} during both dark and light adaptation (79). A therapeutically useful pharmacological agent should decrease Ca^{2+} entry into the cell, decrease entry of Ca^{2+} into the mitochondria, or block the cytochrome c-caspase of apoptosis. Our results with CsA and the nonimmunosuppressive cyclosporin analog NIM811 (64) are consistent with the latter and suggest that NIM811 be tested in animal models of retinal degeneration.

Following the initial report that D-cis diltiazem partially protected rods in the developing retina of $Pde6b^{rd1}$ mice (50), several other laboratories initiated similar studies. Three other studies - one in $Pde6b^{rd1}$ mice, one in $Pde6b^{rcd1}$ dogs and one in Pro23His rats - found no protection with D-cis diltiazem (53-55). The results of our *in vitro* study with low-to-moderate rod Ca^{2+} overload supports these latter findings and of-

fers possible reasons for these results. D-cis diltiazem is a potent inhibitor of the neuronal and rod mitochondrial Na^+/Ca^{2+} exchanger as well as L-type Ca^{2+} channel, however, it is a weak and ineffective racemic inhibitor (compared to L-cis diltiazem) of the rod cGMP-activated conductance. In contrast, L-cis diltiazem is a potent inhibitor of the rod cGMP-activated conductance and a weak inhibitor of the neuronal and rod mitochondrial Na^+/Ca^{2+} exchanger as well as the L-type Ca^{2+} channel (51, 53, 57, 60-62).

Our morphological, biochemical and functional studies with D-cis diltiazem, L-cis diltiazem and verapamil strongly suggest that rod Ca^{2+} overload and subsequent rod-selective apoptosis results from entry of Ca^{2+} through rod cGMP channels - especially in the dark - and not through L-type Ca^{2+} channels present in the rod inner segments and synaptic terminals (70). Therefore, D-cis diltiazem would not be expected to provide neuroprotection from rod Ca^{2+} overload and apoptosis, although L-cis diltiazem was partially effective. Moreover, once excess Ca^{2+} enters the rod mitochondria, inhibition of the mitochondrial Na^+/Ca^{2+} exchanger by D-cis diltiazem could potentiate the apoptotic inducing effects of Ca^{2+} overload by causing further uptake of Ca^{2+} (63) and thus subsequent mPTP opening.

Alternatively, protection from Ca^{2+} overload could be achieved by increasing the mitochondrial buffering capacity of Ca^{2+} (80, 81). Interestingly, Bcl-2 or Bcl-x_L overexpression does not protect rods, neurons and other cells from high Ca^{2+} overload, but does protect them from low-to-moderate Ca^{2+} and/or Pb^{2+} overload (14, 80-84). This approach represents a different avenue for pharmacological therapy.

In conclusion, we established a pathophysiologically-relevant *in vitro* model of low-to-moderate Ca^{2+} overload with subsequent rod-selective apoptosis and then employed five different potential neuroprotective strategies with selected pharmacological agents. The strategies were designed: 1) to block Ca^{2+} entry into rod photoreceptors through the cGMP-activated conductance, 2) to block Ca^{2+} entry into rod photoreceptors through L-type Ca^{2+} channels, 3) to inhibit the rod mitochondrial Na^+/Ca^{2+} exchanger, 4) to inhibit rod mitochondrial cytochrome c release and 5) to inhibit activation of caspase-3 and downstream events. Blockade of Ca^{2+} entry into rods with L-cis diltiazem was partially successful, whereas blockade of Ca^{2+} entry into rod photoreceptors through L-type Ca^{2+} channels with D-cis diltiazem or verapamil was not successful. Inhibition of the mitochondrial Na^+/Ca^{2+} exchanger with D-cis diltiazem also provided no protection. CsA and NIM811, potent inhibitors of the mitochondrial permeability transition pore, blocked all Ca^{2+}-induced apoptosis. The caspase-3 inhibitor DEVD-fmk only blocked the events downstream of cytochrome c-induced apoptosis. Thus, the successful pharmacological neuroprotective strategies for rod Ca^{2+} overload/apoptosis targeted the rod cGMP-activated channels or mPTP, but not the rod L-type Ca^{2+} channels. The mechanistic knowledge gained from these results will hopefully be utilized to develop future successful neuroprotective pharmacological strategies for Ca^{2+} and other divalent cation-induced rod photoreceptor apoptotic cell death.

ACKNOWLEDGEMENTS

Partially funded by NIH Grants ES03183 and EY07024, a Fight-for-Sight Foundation Student Research Grant, a UH PEER Grant, and a College of Optometry VRSG Grant.

Reprint request to:
Donald A. Fox, PhD
College of Optometry
University of Houston
505 J. Davis Armistead Bldg.
Houston, TX - USA 77204-2020
dafox@uh.edu

REFERENCES

1. National Eye Advisory Council Report. 1998. A National Plan: 1999-2003.
2. Thirkill CE, Roth AM, Keltner JL. Cancer-associated retinopathy. Arch Ophthalmol 1987; 105: 372-5.
3. Fox DA, Chu LW. Rods are selectively altered by lead: II. Ultrastructure and quantitative histology. Exp Eye Res 1988; 46: 613-25.

4. Edward DP, Lam TT, Shahinfar S, Li J, Tso MO. Amelioration of light-induced retinal degeneration by a calcium overload blocker: Flunarizine. Arch Ophthalmol 1991; 109: 554-62.
5. Buchi ER. Cell death in rat retina after pressure-induced ischaemia-reperfusion insult: Electron microscopic study. II. Outer nuclear layer. Jpn J Ophthalmol 1992; 36: 62-8.
6. Chang GQ, Hao Y, Wong F. Apoptosis: Final common pathway of photoreceptor death in Rd, Rds, and rhodopsin mutant m. Neuron 1993; 11: 595-605.
7. Portera-Cailliau C, Sung CH, Nathans J, Adler R. Apoptotic photoreceptor cell death in mouse models of retinitis pigmentosa. Proc Natl Acad Sci USA 1994; 91: 974-8.
8. Fox DA, Campbell ML, Blocker YS. Functional alterations and apoptotic cell death in the retina following developmental or adult lead exposure. Neurotoxicology 1997; 18: 645-64.
9. Adamus G, Machnicki M, Elerding H, Sugden B, Blocker YS, Fox DA. Antibodies to recoverin induce apoptosis of photoreceptor and bipolar cells *in vivo*. J Autoimmun 1998; 11: 523-33.
10. van Soest S, Westerveld A, de Jong PT, Bleeker-Wagemakers EM, Bergen AA. Retinitis pigmentosa: Defined from a molecular point of view. Surv Ophthalmol 1999; 43: 321-34.
11. Fox DA, Boyes WK. Ocular and visual system toxicology. In: Klaassen, CD, ed. Casarett & Doull's Toxicology: The Science of Poisons, 6th ed. New York: McGraw-Hill Press 2001; 565-95.
12. Rothenberg SJ, Schnaas L, Salgado-Valladares M, et al. Increased ERG a-wave and b-wave amplitudes in 7- to 10-year old children resulting from prenatal lead exposure. Invest Ophthalmol Vis Sci 2002; 43: 2036-44.
13. Farber DB. From mice to men: the cyclic GMP phosphodiesterase gene in vision and disease. Invest Ophthalmol Vis Sci 1995; 36: 263-75.
14. Fox DA, Poblenz AT, He L. Calcium overload triggers rod photoreceptor apoptotic cell death in chemical-induced and inherited retinal degenerations. Ann N Y Acad Sci 1999; 893: 282-5.
15. Fain GL, Lisman JE. Light, Ca^{2+}, and photoreceptor death: New evidence for the equivalent-light hypothesis From arrestin knockout mice. Invest Ophthalmol Vis Sci 1999; 40: 2770-2.
16. Molday RS. Photoreceptor membrane proteins, phototransduction, and retinal degenerative diseases. Invest Ophthalmol Vis Sci 1998; 39: 2491-513.
17. Huang SH, Pittler SJ, Huang X, Oliveira L, Berson EL, Dryja TP. Autosomal recessive retinitis pigmentosa caused by mutations in the alpha subunit of rod cGMP phosphodiesterase. Nat Genet 1995; 11: 468-71.
18. Dryja TP, Rucinski DE, Chen SH, Berson EL. Frequency of mutations in the gene encoding the alpha subunit of rod cGMP-phosphodiesterase in autosomal recessive retinitis pigmentosa. Invest Ophthalmol Vis Sci 1999; 40: 1859-65.
19. Tsang SH, Gouras P, Yamashita CK, et al. Retinal degeneration in mice lacking the gamma subunit of the rod cGMP phosphodiesterase. Science 1996; 272: 1026-9.
20. Payne AM, Downes SM, Bessant DA, et al. A mutation in guanylate cyclase activator 1A (GUCA1A) in an autosomal dominant cone dystrophy pedigree mapping to a new locus on chromosome 6p21.1. Hum Mol Genet 1998; 7: 273-7.
21. Sokal I, Li N, Surgucheva I, et al. GCAP1 (Y99C) mutant is constitutively active in autosomal dominant cone dystrophy. Mol Cell 1998; 2: 129-33.
22. Downes SM, Holder GE, Fitzke FW, et al. Autosomal dominant cone and cone-rod dystrophy with mutations in the guanylate cyclase activator 1A gene-encoding guanylate cyclase activating protein-1. Arch Ophthalmol 2001; 119: 96-105.
23. McGeoch JE, McGeoch MW, Mao R, Guidotti G. Opposing actions of cGMP and calcium on the conductance of the F(0) subunit c pore. Biochem Biophys Res Commun 2000; 274: 835-40.
24. McGeoch JE, Guidotti G. Batten disease and the control of the F(0) subunit c pore by cGMP and calcium. Eur J Paediatr Neurol 2001: 5 (Suppl A): 147-50.
25. Fox DA, Katz LM, Farber DB. Low level developmental lead exposure decreases the sensitivity, amplitude and temporal resolution of rods. Neurotoxicology 1991; 12: 641-54.
26. Fox DA, Katz LM. Developmental lead exposure selectively alters the scotopic ERG component of dark and light adaptation and increases rod calcium content. Vision Res 1992; 32: 249-55.
27. Srivastava D, Fox DA, Hurwitz RL. Effects of magnesium on cyclic GMP hydrolysis by the bovine retinal rod cyclic GMP phosphodiesterase. Biochem J 1995; 308 (Pt 2): 653-8.
28. Srivastava D, Hurwitz RL, Fox DA. Lead- and calcium-mediated inhibition of bovine rod cGMP phosphodiesterase: interactions with magnesium. Toxicol Appl Pharmacol 1995; 134: 43-52.
29. Fox DA, Rubinstein SD, Hsu P. Developmental lead exposure inhibits adult rat retinal, but not kidney, Na^+, K^+-ATPase. Toxicol Appl Pharmacol 1991; 109: 482-93.
30. Molthagen M, Schachner M, Bartsch U. Apoptotic cell death of photoreceptor cells in mice deficient for the adhesion molecule on glia (AMOG the beta 2- subunit of the Na, K-ATPase). J Neurocytol 1996; 25: 243-55.
31. Weber P, Bartsch U, Schachner M, Montag D. Na, K-ATPase subunit beta1 knock-in prevents lethality of beta2 deficiency in mice. J Neurosci 1998; 18: 9192-203.
32. Wetzel RK, Arystarkhova E, Sweadner KJ. Cellular and subcellular specification of Na, K-ATPase alpha and beta isoforms in the postnatal development of mouse retina. J Neurosci 1999; 19: 9878-89.
33. Szabo ME, Droy-Lefaix MT, Doly M, Braquet P. Ischaemia- and reperfusion-induced Na^+, K^+, Ca^{2+} and Mg^{2+} shifts in rat retina: Effects of two free radical scavengers, SOD and EGB 761. Exp Eye Res 1992; 55: 39-45.

34. Doberstein C, Fineman I, Hovda DA, Martin NA, Keenly L, Becker DP. Metabolic alterations accompany ionic disturbances and cellular swelling during a hypoxic insult to the retina: An *in vitro* study. Acta Neurochir (Wien) 1994; 60 (Suppl): S41-4.
35. Kuriyama H, Nakagawa M, Tsuda M. Intracellular $Ca^{(2+)}$ changes induced by in vitro ischemia in rat retinal slices. Exp Eye Res 2001; 73: 365-74.
36. Reme CE, Grimm C, Hafezi F, Marti A, Wenzel A. Apoptotic cell death in retinal degenerations. Prog Retina Eye Res 1998; 17: 443-64.
37. Phelan JK, Bok D. A brief review of retinitis pigmentosa and the identified retinitis pigmentosa genes. Mol Vis 2000; 6: 116-24.
38. Travis GH. Mechanisms of cell death in the inherited retinal degenerations. Am J Hum Genet 1998; 62: 503-8.
39. Stone J, Maslim J, Valter-Kocsi K, et al. Mechanisms of photoreceptor death and survival in mammalian retina. Prog Retina Eye Res 1999; 18: 689-735.
40. Linden R, Rehen SK, Chiarini LB. Apoptosis in developing retinal tissue. Prog Retina Eye Res 1999; 18: 133-65.
41. Clarke G, Collins RA, Leavitt BR, Andrews DF, Hayden MR, Lumsden CJ, McInnes RR. A one-hit model of cell death in inherited neuronal degenerations. Nature 2000; 406: 195-9.
42. Eversole-Cire P, Chen J, Simon MI. Bax is not the heterodimerization partner necessary for sustained anti-photoreceptor cell death activity of Bcl-2. Invest Ophthalmol Vis Sci 2002; 43: 1636-44.
43. Nicotera P, Orrenius S. The role of calcium in apoptosis. Cell Calcium 1998; 23: 173-80.
44. He, L, Poblenz AT, Medrano CJ, Fox DA. Lead and calcium produce photoreceptor cell apoptosis by opening the mitochondrial permeability transition pore. J Biol Chem 2000; 275: 12175-84.
45. Szabo I, Bernardi P, Zoratti M. Modulation of the mitochondrial megachannel by divalent cations and protons. J Biol Chem 1992; 267: 2940-6.
46. Ichas F, Mazat JP. From calcium signaling to cell death: Two conformations for the mitochondrial permeability transition pore: Switching from low- to high-conductance state. Biochim Biophys Acta 1998; 1366: 33-50.
47. Bernardi P. Mitochondrial transport of cations: channels, exchangers, and permeability transition. Physiol Rev 1999; 79: 1127-55.
48. Pittler SJ, Baehr W. Identification of a nonsense mutation in the rod photoreceptor cGMP phosphodiesterase beta-subunit gene of the rd mouse. Proc Natl Acad Sci USA 1991; 88: 8322-6.
49. Fesenko EE, Kolesnikov SS, Lyubarsky AL. Induction by cyclic GMP of cationic conductance in plasma membrane of retinal rod outer segment. Nature 1985; 313: 310-3.
50. Frasson M, Sahel JA, Fabre M, Simonutti M, Dreyfus H, Picaud S. Retinitis pigmentosa: rod photoreceptor rescue by a calcium-channel blocker in the rd mouse. Nat Med 1999; 5: 1183-7.
51. Ikeda S, Oka J, Nagao T. Effects of four diltiazem stereoisomers on binding of D-cis-[^{3}H]Diltiazem and (+)-[^{3}H]PN200-110 to rabbit T-tubule calcium channels. Eur J Pharmacol 1991; 208: 199-205.
52. Koch KW, Kaupp UB. Cyclic GMP directly regulates a cation conductance in membranes of bovine rods by a cooperative mechanism. J Biol Chem 1985; 260: 6788-800.
53. Pawlyk BS, Li T, Scimeca MS, Sandberg MA, Berson EL. Absence of photoreceptor rescue with D-cis-diltiazem in the rd mouse. Invest Ophthalmol Vis Sci 2002; 43: 1912-5.
54. Pearce-Kelling SE, Aleman TS, Nickle A, et al. Calcium channel blocker D-cis-diltiazem does not slow retinal degeneration in the PDE6B mutant rcd1 canine model of retinitis pigmentosa. Mol Vis 2001; 7: 42-7.
55. Bush RA, Kononen L, Machida S, Sieving PA. The effect of calcium channel blocker diltiazem on photoreceptor degeneration in the rhodopsin Pro213His rat. Invest Ophthalmol Vis Sci 2000; 41: 2697-701.
56. Kueng-Hitz N, Grimm C, Lansel N, Hafezi F, He L, Fox DA, Reme CE, Niemeyer G, Wenzel A. The retina of c-Fos-/- mice: Electrophysiologic, morphologic and biochemical aspects. Invest Ophthalmol Vis Sci 2000; 41: 909-16.
57. Medrano CJ, Fox DA. Substrate-dependent effects of calcium on rat retinal mitochondrial respiration: Physiological and toxicological studies. Toxicol Appl Pharmacol 1994; 125: 309-21.
58. Shulman LM, Fox DA. Dopamine inhibits mammalian photoreceptor Na^+,K^+-ATPase activity via a selective effect on the alpha3 isozyme. Proc Natl Acad Sci USA 1996; 93: 8034-9.
59. Medrano CJ, Fox DA. Oxygen consumption in the rat outer and inner Retina: l. Exp Eye Res 1995; 61: 273-84.
60. Matlib MA, Lee SW, Deprover A, Schwarz A. A specific inhibitory action of certain benzothiazepines and benzodiazepines on the sodium-calcium exchange processes of heart and brain mitochondria. Eur J Pharmacol 1983; 89: 327-8.
61. Cox DA, Matlib MA. Modulation of intramitochondrial free Ca^{2+} concentration by antagonists of Na^+-Ca^{2+} exchange. Trends Pharmacol Sci 1993; 14: 408-13.
62. White RJ, Reynolds IJ. Mitochondria accumulate Ca^{2+} following intense glutamate stimulation of cultured rat forebrain neurones. J Physiol 1997; 498 (Pt 1): 31-47.
63. Vaghy PL, Johnson JD, Matlib MA, Wang T, Schwartz A. Selective inhibition of Na^+-induced Ca^{2+} release from heart mitochondria by diltiazem and certain other Ca^{2+} antagonist drugs. J Biol Chem 1982; 257: 6000-2.
64. Rosenwirth B, Billich A, Datema R, et al. Inhibition of human immunodeficiency virus type 1 replication by SDZ NIM811, a nonimmunosuppressive cyclosporine analog. Antimicrob Agents Chemother 1994; 38: 1763-72.
65. Walmeier PC, Feldtrauer JJ, Qian T, Lemasters JJ. Inhibition of the mitochondrial permeability transition by the nonimmunosuppressive cyclosporin derivative NIM811. Mol Pharmacol 2002; 62: 22-9.

66. Kay JE, Moore AL, Doe SE, Benzie CR, Schonbrunner R, Schmid FX, Halestrap AP. The Mechanism of action of FK506. Transplant Proc 1990; 22: 96-9.
67. Garcia-Calvo M, Peterson EP, Leiting B, Ruel R, Nicholson DW, Thornberry NA. Inhibition of human caspases by peptide-based and macromolecular inhibitors. J Biol Chem 1998; 273: 32608-13.
68. Ratto GM, Payne R, Owen WG, Tsien RY. The concentration of cytosolic free calcium in vertebrate rod outer segments measured with fura-2. J Neurosci 1988; 8: 3240-6.
69. Knopp A, Ruppel H. Ca^{2+} Fluxes and channel regulation in rods of the albino rat. J Gen Physiol 1996; 107: 577-95.
70. Krizaj D, Copenhagen DR. Compartmentalization of calcium extrusion mechanisms in the outer and inner segments of photoreceptors. Neuron 1998; 21: 249-56.
71. Susin SA, Zamzami N, Kroemer G. Mitochondria as regulators of apoptosis: doubt no more. Biochim Biophys Acta 1998; 1366: 151-65.
72. Thornberry NA, Rano TA, Peterson EP, et al .A combinatorial approach defines specificities of members of the caspase family and granzyme B: Functional relationships established for key mediators of apoptosis. J Biol Chem 1997; 272: 17907-11.
73. Talanian RV, Quinlan C, Trautz S, et al. Substrate specificities of caspase family proteases. J Biol Chem 1997; 272: 9677-82.
74. Stennicke HR, Salvesen GS. Biochemical characteristics of caspases-3, -6, -7, and -8. J Biol Chem 1997; 272: 25719-23.
75. Ikonomidou C, Mosinger JL, Salles KS, Labruyere J, Olney JW. Sensitivity of the developing rat brain to hypobaric/ischemic damage parallels sensitivity to N-methyl-aspartate neurotoxicity. J Neurosci 1989; 9: 2809-18.
76. Mundy WR, Freudenrich TM. Sensitivity of immature neurons in culture to metal-induced changes in reactive oxygen species and intracellular free calcium. Neurotoxicology 2000; 21: 1135-44.
77. Franklin JL, Johnson EM, Jr. Block of neuronal apoptosis by a sustained increase of steady-state free Ca^{2+} concentration. Philos Trans R Soc Lond B Biol Sci 1994; 345: 251-6.
78. Shiells RA, Falk G. Properties of the cGMP-activated channel of retinal on-bipolar cells. Proc R Soc Lond B Biol Sci 1992; 247: 21-5.
79. Somlyo AP, Walz B. Elemental distribution in Rana pipiens retinal rods: Quantitative electron probe analysis. J Physiol 1985; 358: 183-95.
80. Murphy AN, Bredesen DE, Cortopassi G, Wang E, Fiskum G. Bcl-2 potentiates the maximal calcium uptake capacity of neural cell mitochondria. Proc Natl Acad Sci USA 1996; 93: 9893-8.
81. Zhu L, Ling S, Yu XD, Venkatesh LK, Subramanian T, Chinnadurai G, Kuo TH. Modulation of mitochondrial Ca^{2+} homeostasis by Bcl-2. J Biol Chem 1999; 274: 33267-73.
82. Chen J, Flannery JG, LaVail MM, Steinberg RH, Xu J, Simon MI. Bcl-2 overexpression reduces apoptotic photoreceptor cell death in three different retinal degenerations. Proc Natl Acad Sci USA 1996; 93: 7042-7.
83. Joseph RM, Li T. Overexpression of Bcl-2 or Bcl-x_L transgenes and photoreceptor degeneration. Invest Ophthalmol Vis Sci 1996; 37: 2434-46.
84. He L, Perkins GA, Poblenz AT, Harris JB, Hung M, Ellisman MH, Fox DA. Bcl-x_L over expression blocks bax-mediated mitochondrial contact site formation and apoptosis in rod photoreceptors of lead-exposed mice. Proc Natl Acad Sci USA 2003; 100: 1022-7.